

DOI: 10.1002/cssc.201402402

Iron Oxide Encapsulated by Ruthenium Hydroxyapatite as Heterogeneous Catalyst for the Synthesis of 2,5-Diformylfuran

Zehui Zhang,* Ziliang Yuan, Dingguo Tang, Yongshen Ren, Kangle Lv, and Bing Liu^[a]

Magnetic γ -Fe₂O₃ nanocrystallites encapsulated by hydroxyapatite (HAP), HAP@ γ -Fe₂O₃, were prepared followed by cation exchange of Ca²⁺ on the external HAP surface with Ru³⁺ to give the γ -Fe₂O₃@HAP-Ru catalyst. The structure of the as-prepared catalyst was characterized, and its catalytic activity was studied in the aerobic oxidation of 5-hydroxymethylfurfural (HMF). γ -Fe₂O₃@HAP-Ru showed a high catalytic activity for the aerobic oxidation of HMF into 2,5-diformylfuran (DFF). A high DFF yield of 89.1% with an HMF conversion of 100% was obtained after 4 h at 90 °C. Importantly, the synthesis of DFF from fruc-

tose was realized by two consecutive steps. The dehydration of fructose in the presence of a magnetic acid catalyst (Fe₃O₄@SiO₂-SO₃H) produced HMF in a yield of 90.1%. Then the Fe₃O₄@SiO₂-SO₃H catalyst was removed from the reaction solution with a permanent magnet, and HMF in the resulting solution was further oxidized to DFF with a yield of 79.1% based on fructose. The synthesis of DFF from fructose by two steps avoids the tedious separation of the intermediate HMF, which saves time and energy.

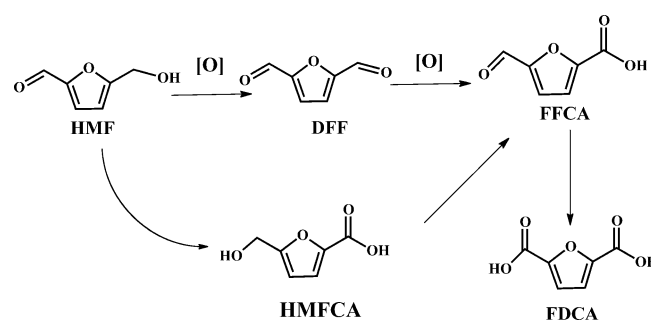
Introduction

The growing concern over the depletion of fossil fuel has resulted in a growing interest in the production of energy and chemicals from renewable resources.^[1–3] Although renewable energy can be produced from renewable sources such as wind, solar, and geothermal, none of these renewable sources can be used to produce organic chemicals. Biomass is the only carbon-containing renewable resource and it is attractive as a feedstock for energy and the chemical industry.^[4–6] In this context, much effort has been devoted to the transformation of abundant biomass resources into chemicals and liquid fuels.

5-Hydroxymethylfurfural (HMF), the acid-catalyzed dehydration product of C₆-based carbohydrates, has two functionalities attached to a furan ring. It can be used as a versatile precursor for the synthesis of transportation fuels, pharmaceuticals, and other petroleum-derived chemicals.^[7,8] Therefore, there has been an overwhelming interest in the synthesis of HMF from monosaccharides, polysaccharides, cellulose, and lignocelluloses.^[9–13]

Recently, the oxidation of HMF has received increasing attention. The oxidation of HMF can generate several kinds of oxidation products such as 2,5-diformylfuran (DFF), 5-hydroxymethyl-2-furancarboxylic acid (HMFCA), 5-formyl-2-furancarboxylic acid (FFCA), and 2,5-furandicarboxylic acid (FDCA;

Scheme 1). FDCA is a highly promising bio-based building block for resins and polymers, thus it can be used as a promising replacement for terephthalic acid (TA), a petroleum-based



Scheme 1. Oxidation products of HMF.

monomer in the plastics industry.^[14,15] DFF is another important oxidation product of HMF that is useful in many fields, such as the synthesis of Schiff bases, pharmaceuticals, antifungal agents, and organic conductors.^[16–18]

Early reports on the oxidation of HMF into DFF focused mainly on classic oxidation methods, which had some drawbacks such as their high cost and the production of large amounts of waste.^[19,20] Therefore, the development of environmentally friendly methods for the oxidation of HMF into DFF with O₂ is required. Some homogeneous catalysts have been used for the aerobic oxidation of HMF into DFF,^[21–23] but the major drawback of homogeneous catalysts is the difficulty of their recovery. Therefore, the aerobic oxidation of HMF with heterogeneous catalysts is an intriguing prospect in biorefineries. Recently, some heterogeneous catalytic systems have been

[a] Prof. Z. H. Zhang, Z. L. Yuan, Dr. D. G. Tang, Dr. Y. S. Ren, Dr. K. L. Lv, Dr. B. Liu
Key Laboratory of Catalysis and Material Sciences
State Ethnic Affairs Commission & Ministry of Education
South-Central University for Nationalities
MinYuan Road 182, Wuhan (PR China)
Fax: (+86) 27-67842752
E-mail: zehuizh@mail.ustc.edu.cn

reported for the aerobic oxidation of HMF into DFF.^[24–26] Although heterogeneous catalysts can be recycled, their tedious recovery by filtration or centrifugation and the inevitable loss of solid catalysts during the separation process still limit their application.

Recently, magnetic materials have opened up a new avenue to introduce efficient systems to facilitate catalyst recovery in different liquid-phase reactions.^[27] Iron oxides are usually used as magnetic materials but they tend to aggregate. It has been demonstrated that the encapsulation of iron oxide nanoparticles prevents their aggregation and improves their stability. Recently, γ -Fe₂O₃ encapsulated by hydroxyapatite (HAP), γ -Fe₂O₃@HAP, as a magnetic support has been used to construct various catalysts for many chemical reactions.^[28,29] For example, Sheykhan et al.^[29] prepared *n*-propyl sulfamic acid covalently supported on hydroxyapatite-encapsulated magnetic nanoparticles for the Friedländer reaction. One important characteristic of HAP is that Ca²⁺ in its framework can be exchanged with other metal cations, which allows the introduction of active sites. It was reported that Ru-exchanged hydroxyapatite (HAP-Ru) showed a high catalytic activity in the oxidation of alcohols with O₂.^[30] Herein, HAP-Ru-encapsulated magnetic γ -Fe₂O₃ (γ -Fe₂O₃@HAP-Ru) was prepared and used for the oxidation of HMF into DFF with O₂. Importantly, a magnetic acid catalyst functionalized with sulfonic acid (Fe₃O₄@SiO₂-SO₃H) was also prepared and used to catalyze the dehydration of fructose into HMF. The resulting reaction solution was used directly without separation for the synthesis of DFF by the in situ oxidation of HMF without the need to purify the HMF.

Results and Discussion

Catalyst preparation and characterization

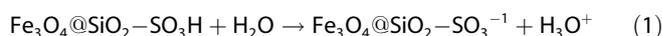
The procedures for the synthesis of the γ -Fe₂O₃@HAP-Ru catalyst are shown in Scheme 2A. The coprecipitation of Fe²⁺ and Fe³⁺ ions in alkaline solution under a N₂ atmosphere produced Fe₃O₄ nanoparticles. The Fe₃O₄ nanoparticles were then coated with HAP, which was formed from Ca²⁺ and PO₄³⁻ at pH 11. The resultant material was calcined at 300 °C for 3 h to give the γ -Fe₂O₃@HAP support. Finally, γ -Fe₂O₃@HAP was stirred in an aqueous solution of RuCl₃ at room temperature to produce the γ -Fe₂O₃@HAP-Ru catalyst. During the cation-exchange process, the black solution became clear, and the content of Ru

was determined to be 2.0 wt% by inductively coupled plasma atomic emission spectroscopy (ICP-AES).

The Ru dispersion was calculated from H₂ temperature-programmed desorption (H₂-TPD) measured by using a Zeton Altomare AMI-200 unit. The γ -Fe₂O₃@HAP-Ru (50 mg) catalyst was reduced at 350 °C for 12 h using a flow of high-purity H₂ and then cooled to 100 °C under a H₂ stream. The sample was held at 100 °C for 1 h under flowing Ar to remove weakly bound physisorbed species prior to increasing the temperature slowly to 350 °C. At this temperature, the catalyst was held under flowing Ar to desorb the remaining chemisorbed hydrogen, and the thermal conductivity detector (TCD) recorded the signal until it returned to the baseline. The chemisorbed H₂ uptake at 100 °C was determined to be 82.7 $\mu\text{mol}_{\text{H}_2}\text{g}^{-1}$ catalyst. According to the chemisorption stoichiometry H/Ru = 1:1,^[31] the Ru dispersion was determined to be 83.5%, which indicated that the Ru was exchanged well with the surface Ca²⁺.

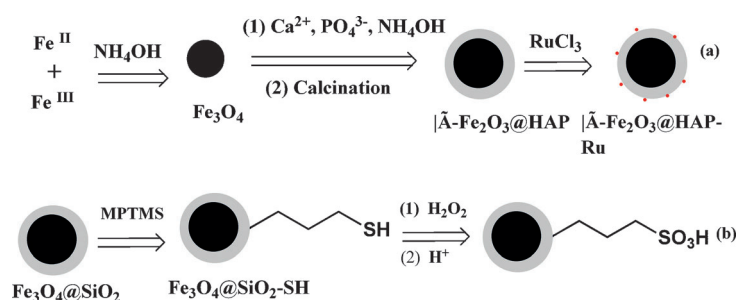
The procedure for the synthesis of Fe₃O₄@SiO₂-SO₃H is shown in Scheme 2B. The core-shell silica-coated Fe₃O₄ nanoparticles (Fe₃O₄@SiO₂) were prepared according to our previous work.^[27] The surface of Fe₃O₄@SiO₂ was then grafted with γ -mercaptopropyl groups. Finally, the thiol groups in Fe₃O₄@SiO₂-SH were oxidized to sulfonic acid groups by H₂O₂ to obtain the Fe₃O₄@SiO₂-SO₃H acid catalyst.

The amount of H⁺ in Fe₃O₄@SiO₂-SO₃H was determined by an acid-base titration method according to Equation (1). The liberated H₃O⁺ was titrated by standard NaOH. The amount of H⁺ in the Fe₃O₄@SiO₂-SO₃H catalyst was determined to be 0.9 mmol g⁻¹.



Fe₃O₄@SiO₂-SO₃H and γ -Fe₂O₃@HAP-Ru were characterized by XRD, and the results are shown in Figure 1. Characteristic diffraction peaks for the Fe₃O₄@SiO₂-SO₃H sample were observed clearly at $2\theta = 30.2, 35.4, 43.3, 53.7, 57.3,$ and 62.9° (Figure 1A), which are attributed to the (220), (311), (400), (422), (511), and (440) Bragg reflections of the face-centered cubic lattice of Fe₃O₄ nanoparticles, respectively (JCPDS No. 19-0629). In the XRD pattern of γ -Fe₂O₃@HAP-Ru, peaks at $2\theta = 35.8, 43.7, 53.7, 57.3,$ and 63.0° were assigned to the reflections of γ -Fe₂O₃.^[28] Furthermore, several well-resolved diffraction peaks at $2\theta = 25.9, 31.8, 32.9, 34.1, 39.8, 46.7,$ and 49.5° were observed clearly in the pattern of γ -Fe₂O₃@HAP-Ru, which were characteristic of HAP.^[28] The XRD results indicated that γ -Fe₂O₃ nanoparticles were encapsulated successfully with HAP.

FTIR spectra of Fe₃O₄@SiO₂-SO₃H and γ -Fe₂O₃@HAP-Ru are shown in Figure 2. The spectrum of Fe₃O₄@SiO₂-SO₃H was similar to that seen in the literature for silica-supported alkyl sulfonic acids.^[32] A broad peak at $\tilde{\nu} = 3000\text{--}3700\text{ cm}^{-1}$ centered around $\tilde{\nu} = 3400\text{ cm}^{-1}$ and a sharper peak at $\tilde{\nu} = 1640\text{ cm}^{-1}$ were observed, which are assigned to the O-H stretching vibration of surface hydroxyl groups and physisorbed water, respectively.^[32] An intense peak around $\tilde{\nu} = 1040\text{ cm}^{-1}$ was attributed to the asymmetric Si-



Scheme 2. Preparation of (a) γ -Fe₂O₃@HAP-Ru and (b) Fe₃O₄@SiO₂-SO₃H.

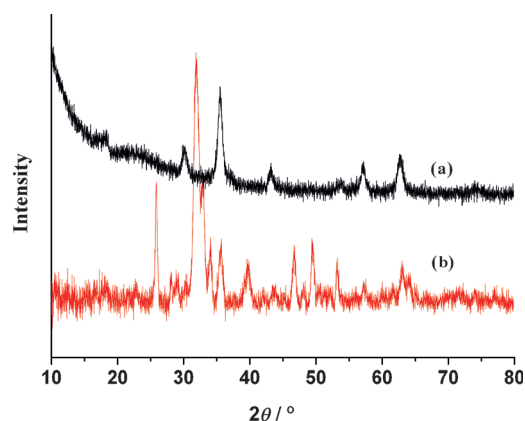


Figure 1. XRD patterns of (a) $\text{Fe}_3\text{O}_4@SiO_2-SO_3H$ and (b) $\gamma\text{-Fe}_2O_3@HAP\text{-Ru}$.

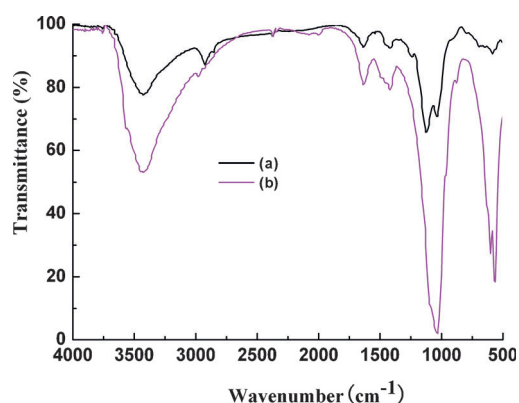


Figure 2. FTIR spectra of (a) $\text{Fe}_3\text{O}_4@SiO_2-SO_3H$ and (b) $\gamma\text{-Fe}_2O_3@HAP\text{-Ru}$.

O–Si stretching vibration, and a weak peak at $\tilde{\nu}=800\text{ cm}^{-1}$ was caused by the symmetric Si–O–Si stretching vibration. The presence of surface organic functional groups in the $\text{Fe}_3\text{O}_4@SiO_2-SO_3H$ catalyst was proved clearly by FTIR spectroscopy. The C–H stretch and C–H bending vibrations are visible at $\tilde{\nu}=2920$ and 1420 cm^{-1} , respectively. The FTIR absorption of the O=S=O asymmetric and symmetric stretching modes was at $\tilde{\nu}=1240$ and 1123 cm^{-1} , respectively, and that of the S–O stretching mode appeared at $\tilde{\nu}=647\text{ cm}^{-1}$.^[33] In addition, a peak at $\tilde{\nu}=587\text{ cm}^{-1}$ was also observed, which was assigned to Fe–O vibrations of the Fe_3O_4 core in the $\text{Fe}_3\text{O}_4@SiO_2-SO_3H$ catalyst.^[34]

The FTIR spectrum of $\gamma\text{-Fe}_2O_3@HAP\text{-Ru}$ is shown in Figure 2B. The characteristic $\nu(\text{OH})$ vibrations of lattice hydroxyl groups at $\tilde{\nu}=3570$ and 640 cm^{-1} were observed, which were produced by HAP.^[35] A broad peak centered around $\tilde{\nu}=3400^{-1}$ and a peak at $\tilde{\nu}=1640\text{ cm}^{-1}$ are attributed to adsorbed water.^[35] The asymmetric and symmetric stretching modes of PO_4^{3-} groups were observed at $\tilde{\nu}=1100, 1045, 960, 600,$ and 565 cm^{-1} .^[35] The characteristic stretching vibration of the Fe–O bond at $\tilde{\nu}=598\text{ cm}^{-1}$ overlapped with one of the stretching vibrations of PO_4^{3-} .^[36] The band at $\tilde{\nu}=875\text{ cm}^{-1}$ indicated that HPO_4^{2-} was present in the catalyst as an impurity.^[37] In addition, carbonate impurities in the catalyst were identified by a set of signals in the $\tilde{\nu}=1600\text{--}1300\text{ cm}^{-1}$ region, which originate from CO_2 adsorption from air during sample handling.^[38]

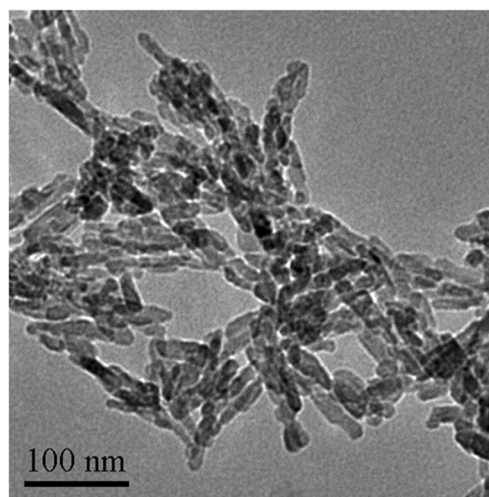


Figure 3. TEM image of $\gamma\text{-Fe}_2O_3@HAP\text{-Ru}$.

TEM images of the as-prepared $\gamma\text{-Fe}_2O_3@HAP\text{-Ru}$ catalyst are shown in Figure 3. The as-synthesized $\gamma\text{-Fe}_2O_3@HAP\text{-Ru}$ has a spindle-shaped morphology. In addition, slight aggregation was observed in the TEM images. $\gamma\text{-Fe}_2O_3$ is visible in the center of the $\gamma\text{-Fe}_2O_3@HAP\text{-Ru}$ (dark spots). The results indicate that $\gamma\text{-Fe}_2O_3$ was encapsulated by HAP. The encapsulation of $\gamma\text{-Fe}_2O_3$ by HAP was verified by X-ray photoelectron spectroscopy (XPS), in which no XPS peaks for Fe were observed. The XPS results also indicated that $\gamma\text{-Fe}_2O_3$ was encapsulated by HAP.

The surface composition of $\gamma\text{-Fe}_2O_3@HAP\text{-Ru}$ was also studied by XPS. The survey scan XPS spectrum of $\gamma\text{-Fe}_2O_3@HAP\text{-Ru}$ (Figure 4a) shows peaks that correspond to the HAP framework elements (Ca, P, O) and Ru. It was reported the broadening of the $\text{Fe}2p_{1/2}$ peak (binding energy, $\text{BE}\approx 711\text{ eV}$) and $\text{Fe}2p_{3/2}$ peak ($\text{BE}\approx 724\text{ eV}$) at high energy is characteristic of Fe^{2+} in Fe_2O_3 .^[39] There were no peaks at $\text{BE}\approx 711$ and 724 eV . These results also indicated that $\gamma\text{-Fe}_2O_3$ was successfully encapsulated by HAP.

To gain an insight into the valence state of the Ru species in the $\gamma\text{-Fe}_2O_3@HAP\text{-Ru}$ framework, high-resolution XPS of Ru 3p and Ru 3d were measured (Figure 4b and c, respectively). The C 1s peak was taken as the reference at $\text{BE}=284.9\text{ eV}$. The Ru $3d_{3/2}$ signal was overlapped completely with the C 1s signal, but the Ru $3d_{5/2}$ peak was discerned at $\text{BE}=281.9\text{ eV}$. Metallic Ru⁰ invariably has binding energies at $279.8\pm 0.2\text{ eV}$, for RuO_2 peaks at $\text{BE}=281$ and 282.1 eV are found, and RuCl_3 has a characteristic peak at $\text{BE}=281.8\text{ eV}$.^[40] The peak at $\text{BE}=281.9\text{ eV}$ observed for Ru $3d_{5/2}$ indicated clearly that the Ru in $\gamma\text{-Fe}_2O_3@HAP\text{-Ru}$ is in an oxidized state, probably Ru³⁺ or Ru⁴⁺. To differentiate between Ru³⁺ and Ru⁴⁺, the Ru $3p_{3/2}$ spectrum of $\gamma\text{-Fe}_2O_3@HAP\text{-Ru}$ was also collected. The Ru $3p_{3/2}$ peak was observed at $\text{BE}=463.2\text{ eV}$ (Figure 4c), which is similar to that of Ru–HAP prepared conventionally that involves Ru^{III} species. In addition, it was reported that the Ru $3p_{3/2}$ peak with Ru^{IV} was up to $\text{BE}=465.2\text{ eV}$, which was higher than the value of $\text{BE}=463.2\text{ eV}$ for Ru^{III} species.^[41] The valence state of Ru in $\gamma\text{-Fe}_2O_3@HAP\text{-Ru}$ was consistent with the results reported by

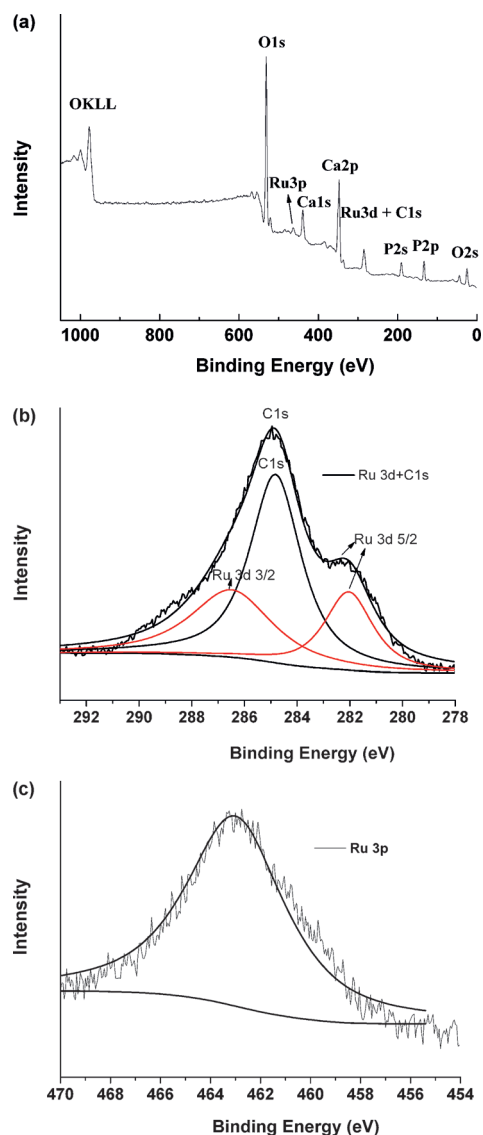


Figure 4. XPS spectra of the samples: (a) Survey scan of $\gamma\text{-Fe}_2\text{O}_3\text{@HAP-Ru}$, (b) Ru 3d region, and (c) Ru 3p region.

Wuyts et al.^[42] They confirmed that the oxidation state of Ru in Ru-HAP was Ru^{III} , in which the method for the preparation of Ru-HAP was similar to ours by stirring the HAP in RuCl_3 solution.

It is important that the prepared catalyst should possess sufficient paramagnetic properties for practical applications. Magnetic hysteresis was measured for the $\gamma\text{-Fe}_2\text{O}_3\text{@HAP-Ru}$ catalyst in an applied magnetic field at 300 K with the field sweeping from -4000 to $+4000$ Oe. The isothermal magnetization curve of $\gamma\text{-Fe}_2\text{O}_3\text{@HAP-Ru}$ at 300 K displayed a rapid increase with the increasing applied magnetic field because of superparamagnetic relaxation (Figure 5). The saturation magnetization reached 6.1 emu g^{-1} . The magnetization is sufficient for magnetic separation by a permanent magnet.

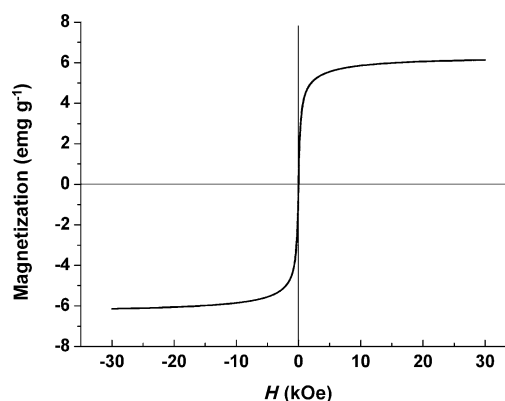


Figure 5. Hysteresis loops for the $\gamma\text{-Fe}_2\text{O}_3\text{@HAP-Ru}$ catalyst at 300 K.

Effect of the solvents on the aerobic oxidation of HMF

To find a suitable solvent for the aerobic oxidation of HMF, some common organic solvents and water were tested (Table 1). HMF conversion and DFF selectivity were affected greatly by the solvent. Although both DMSO and DMF are strongly polar solvents with high boiling points, a higher HMF conversion was obtained in DMSO than in DMF (Table 1, entries 1 and 2). The $\gamma\text{-Fe}_2\text{O}_3\text{@HAP-Ru}$ catalyst showed high catalytic activity in aromatic solvents such as toluene, trifluorotoluene, and 4-chlorotoluene (Table 1, entries 3–5). The best result was obtained if the oxidation of HMF was performed in 4-chlorotoluene (Table 1, entry 5). An HMF conversion of 100% and a DFF yield of 81.4% were obtained in 4-chlorotoluene after 2 h (Table 1, entry 5). A moderate HMF conversion of 47.5% was obtained in methyl isobutyl ketone (MIBK), but it gave the highest selectivity to DFF in 85.0% (Table 1, entry 6). As MIBK is usually used as an organic extractant in biphasic systems (MIBK/water) for the conversion of fructose into HMF, our method shows the potential for the synthesis of DFF from fructose by two consecutive steps, which comprise the production of HMF from fructose in a biphasic system (MIBK/water) and the subsequent oxidation of HMF in MIBK. Poor results were obtained if reactions were performed in low-boiling-

Entry	Solvent	$\varepsilon/\varepsilon_0$ (25 °C), Ref. [43]	t [h]	HMF conversion [%]	DFF yield [%]	DFF selectivity [%]
1	DMF	37.0	12	36.6	27.9	76.2
2	DMSO	46.7	12	82.4	58.9	71.5
3	toluene	2.4	4	98.1	68.3	69.4
4	benzotrifluoride	–	2	97.6	80.3	82.3
5	4-chlorotoluene	–	2	100	81.4	81.4
6	MIBK	–	12	47.5	40.4	85.0
7	acetonitrile	37.5	12	17.5	10.1	57.7
8	ethanol	24.5	12	23.7	15.8	66.6
9	water	80.1	12	17.7	10.7	60.5

[a] Reaction conditions: $\gamma\text{-Fe}_2\text{O}_3\text{@HAP-Ru}$ (150 mg), HMF (100 mg), 110 °C, solvent (7 mL), O_2 (20 mL min^{-1}).

point solvents such as acetonitrile and ethanol (Table 1, entries 7 and 8). A poor catalytic performance was also observed if the oxidation of HMF was conducted in water (Table 1, entry 9).

Generally, the reaction solvent showed a remarkable effect on chemical reactions. The nature of these solvent effects is complicated because of their dependence on the catalyst properties and reaction conditions and their origin remains unclear.^[44] In addition, the properties of the solvent, such as the polarity, dielectric constant, steric hindrance, and acid–base properties, also have a great effect on the chemical reaction. The aerobic oxidation of HMF over $\gamma\text{-Fe}_2\text{O}_3\text{@HAP-Ru}$ did not seem to follow any trend in terms of solvent dielectric constant (a relative measure of the solvent polarity; Table 1), which suggested that the effect of the solvent on the $\gamma\text{-Fe}_2\text{O}_3\text{@HAP-Ru}$ -catalyzed oxidation of HMF was more than a polar effect. Interestingly, solvents that contain heteroatoms (N, O) led to lower HMF conversions and DFF yields than aromatic solvents. One possible reason is the stronger interactions between the solvent (the heteroatoms N, O as the electron donor) and the catalytic center (Ru as the electron acceptor). This phenomenon was also observed by Lignier et al. who used Au/TiO₂ for the oxidation of alcohols.^[45] They found that solvents that did not contain heteroatoms (N, O, S) resulted in significant product yields. In addition, our results also were consistent with previous results, in which HAP-supported Ru catalysts showed a high catalytic activity in aromatic solvents for the oxidation of alcohols.^[46]

Effect of reaction temperature on the aerobic oxidation of HMF

The effect of the reaction temperature on the aerobic oxidation of HMF into DFF was studied over $\gamma\text{-Fe}_2\text{O}_3\text{@HAP-Ru}$ in 4-chlorotoluene (Table 2). Higher reaction temperatures led to higher HMF conversions. Only 2 h was needed to obtain an HMF conversion of 100% with a DFF yield of 81.4% at 110 °C. If the reaction temperature decreased to 90 °C, a longer reaction time of 4 h was required to obtain a 100% HMF conversion with a DFF yield of 89.1% (Table 2, entries 1 and 2). FDCA was the main byproduct, which was formed by the further oxidation of DFF. Interestingly, the oxidation reaction could proceed smoothly at a low temperature of 70 °C, but a long reaction time was required to obtain a high HMF conversion (Table 2, entries 4 and 5). An HMF conversion of 100% and a DFF yield of 83.4% were obtained after 14 h at 70 °C (Table 2, entry 5). A moderate HMF conversion of 41.5% and a DFF yield of 36.6% were obtained after 12 h at 50 °C (Table 2, entry 6), whereas the oxidation of HMF hardly occurred at room temperature (Table 2, entry 7). In addition, as the reaction comprised the oxidation of HMF into DFF and the subsequent oxidation of DFF into FDCA, the selectivity of DFF depended on both the reaction tempera-

Table 2. Results of the aerobic oxidation of HMF into DFF catalyzed by $\gamma\text{-Fe}_2\text{O}_3\text{@HAP-Ru}$ at different reaction temperatures.^[a]

Entry	T [°C]	t [h]	HMF conversion [%]	DFF yield [%]	DFF selectivity [%]	FDCA yield [%]
1	110	2	100	81.4	81.4	13.9
2	90	4	100	89.1	89.1	9.3
3	70	4	43.2	38.3	88.6	2.2
4	70	12	97.5	84.8	86.9	6.8
5	70	14	100	83.4	83.4	9.7
6	50	12	41.5	36.6	88.1	3.7
7	25	12	11.4	10.7	93.8	0.4

[a] Reaction conditions: $\gamma\text{-Fe}_2\text{O}_3\text{@HAP-Ru}$ (150 mg), HMF (100 mg), 4-chlorotoluene (7 mL), O₂ (20 mL min⁻¹).

ture and the reaction time. With the same HMF conversion of 100%, the lowest selectivity of DFF (81.4%) was obtained in 2 h at 110 °C (Table 2, entry 1), which indicates that a high reaction temperature benefited the subsequent oxidation of DFF into FDCA. The highest selectivity of DFF was obtained in 89.1% at 90 °C after 4 h (Table 2, entry 2). If the reaction temperature was further decreased to 70 °C, a long reaction time of 14 h was needed to achieve full HMF conversion, but the selectivity was moderate (Table 2, entry 5).

Effect of the catalyst amount on the aerobic oxidation of HMF

The results of the aerobic oxidation of HMF into DFF with different amounts of $\gamma\text{-Fe}_2\text{O}_3\text{@HAP-Ru}$ are shown in Table 3. The HMF conversion and DFF yield increased with the increase of the catalyst amount at the same reaction time point. For example, HMF conversions reached 27.5, 51.9, and 100% after 4 h with the catalyst amounts of 25, 50, and 100 mg, respectively, and the corresponding DFF yields were 24.3, 45.9, and 83.4%, respectively (Table 3, entries 1–3). The increased HMF conversion with an increase of the catalyst amount in the same reaction time period is attributed to an increase in the availability and number of catalytically active sites. However, the selectivity of DFF was not affected notably by the catalyst amount

Table 3. Results of the aerobic oxidation of HMF into DFF with different amounts of $\gamma\text{-Fe}_2\text{O}_3\text{@HAP-Ru}$.^[a]

Entry	Catalyst amount [mg]	t [h]	HMF conversion [%]	DFF yield [%]	DFF selectivity [%]	TON
1	25	4	27.5	24.3	87.4	44.1
2	50	4	51.9	45.9	88.6	41.6
3	100	4	100	83.4	83.4	40.1
4	150	2	100	81.4	81.4	26.7
5	without catalyst	4	2.7	0	0	–
6 ^[b]	150	4	3.1	0	0	–
7 ^[c]	100	4	74.2	65.1	87.7	29.7
8 ^[c]	100	8	100.0	84.9	84.9	40.1
9 ^[d]	100	12	82.7	65.6	79.3	33.2

[a] Reaction conditions: A set amount of $\gamma\text{-Fe}_2\text{O}_3\text{@HAP-Ru}$, HMF (100 mg), 4-chlorotoluene (7 mL), 110 °C, O₂ (20 mL min⁻¹). [b] 150 mg of $\gamma\text{-Fe}_2\text{O}_3\text{@HAP}$ was used. [c] Under O₂ balloon. [d] In air.

(Table 3, entries 1–3). With a further increase of the catalyst amount to 150 mg, a short reaction time of 2 h was enough to obtain an HMF conversion of 100% and a DFF yield of 81.4% (Table 3, entry 4).

The turnover number (TON) of the oxidation of HMF over γ -Fe₂O₃@HAP-Ru was calculated (Table 3). In contrast to the trend of the HMF conversion and DFF yield, the TON decreased with the increase of the catalyst amount. Unlike chemical reactions with homogeneous catalysts, liquid-phase reactions with heterogeneous catalysts are limited by mass transfer in the reaction system. The substrate (HMF) in the liquid solution is required to reach the active sites (Ru). With the same HMF concentration, a larger amount of the catalyst resulted in the slower mass transfer of the substrate from the liquid solution to the active sites. Therefore, the TON decreased with the increase of the catalyst amount under the otherwise same conditions, which means that the reaction results are a convolution of kinetics and mass transfer. Control experiments were performed without catalyst or in the presence of γ -Fe₂O₃@HAP, and no DFF was determined in both cases (Table 3, entries 5 and 6). These results indicated that the Ru species were the active sites for the aerobic oxidation of HMF into DFF.

The high catalytic activity of γ -Fe₂O₃@HAP-Ru inspired us to perform the oxidation of HMF under less rigorous conditions. Therefore, reactions were performed under an O₂ balloon or in air (Table 3, entries 7–9). An HMF conversion of 100% and a DFF yield of 84.9% were obtained after 8 h under an O₂ balloon (Table 3, entry 8). Good results were also achieved if the reaction was conducted in air (Table 3, entry 9). The high catalytic activity of γ -Fe₂O₃@HAP-Ru under an O₂ balloon or in air makes this method much more attractive in practical applications from an economical viewpoint because of the mild operation conditions.

Time course of the product distribution

To gain more insight into the oxidation of HMF into DFF, the time course of HMF recovery and product yields were recorded (Figure 6). The content of HMF decreased gradually during the reaction process, and the DFF yield increased gradually from 31.4% after 2 h to 84.8% after 12 h. Furthermore, FDCA and HMFCFA were determined as the byproducts of the reaction in

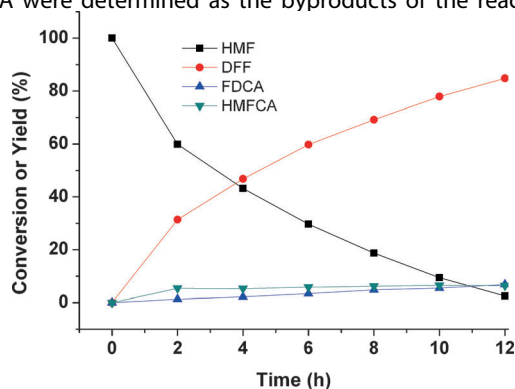


Figure 6. Time course of the product distribution. Reaction conditions: γ -Fe₂O₃@HAP-Ru (150 mg), HMF (100 mg), 4-chlorotoluene (7 mL), O₂ (20 mL min⁻¹), 70 °C.

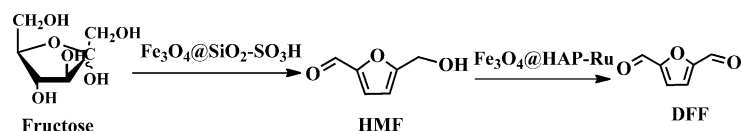
low yields. The FDCA and HMFCFA yields were 6.8 and 6.4%, respectively, after 12 h. The total yield of DFF, FDCA, and HMFCFA after 12 h was close to the conversion of HMF, which indicated that no other byproducts were formed in the aerobic oxidation of HMF.

Interestingly, it was found that HMFCFA was formed mostly at the beginning of the experiment, whereas the yields of both FDCA and DFF increased linearly. The oxidation of the hydroxyl group in HMF produces DFF (this is the main reaction in our case), and the oxidation of the aldehyde group in HMF produces HMFCFA (one of the minor byproducts in our case; Scheme 1). Both DFF and HMFCFA can be further converted into FDCA. FDCA was also detected as one of the minor byproducts in our case. Therefore, according to the reaction routes of HMF, it is not difficult to understand why HMFCFA was formed mostly at the beginning of the experiment and why the yields of both FDCA and DFF increased linearly. DFF is the major product, the yield of which increased with the increase of the reaction time. FDCA was the final oxidation product, the yield of which also increased during the reaction process as it can be produced from the oxidation of DFF or HMFCFA. The yield of HMFCFA fluctuated at a level of 6% after the beginning of the reaction. The reasons might be that HMFCFA was not formed mainly from HMF and that the HMFCFA formed during the reaction was further converted into FDCA.

Synthesis of DFF from fructose through two consecutive steps

As the aerobic oxidation of HMF over γ -Fe₂O₃@HAP-Ru gave an excellent DFF yield, we tried to obtain DFF directly from fructose in the presence of the binary catalysts, namely, Fe₃O₄@SiO₂-SO₃H and γ -Fe₂O₃@HAP-Ru, in which Fe₃O₄@SiO₂-SO₃H was used to catalyze the dehydration of fructose into HMF and γ -Fe₂O₃@HAP-Ru was used for the in situ oxidation of HMF into DFF. 4-Chlorotoluene was the best solvent for the aerobic oxidation of HMF into DFF, and DMSO was a superior organic solvent for the dehydration of fructose into HMF.^[47] Therefore, a mixture of DMSO and 4-chlorotoluene (1:4 v/v) was used as the solvent for the synthesis of DFF from fructose through two consecutive steps.

Initially, the one-step conversion of fructose into DFF was performed in the presence of Fe₃O₄@SiO₂-SO₃H and γ -Fe₂O₃@HAP-Ru under O₂. However, the one-step reaction resulted in very low yields of HMF (1.4%) and DFF (3.5%) at 110 °C after 4 h. Our results were consistent with those reported recently on the synthesis of DFF from fructose in one step using two binary catalysts.^[48] The low DFF yield from fructose in a one-step reaction was mainly because of the possible oxidation of fructose, which results in undesired byproducts. For example, Heinen et al.^[49] reported that the oxidation of fructose with O₂ on Pt/C catalysts formed two major products, 2-keto-D-gluconic acid and D-threo-hexo-2,5-diulose (5-ketofructose). Therefore, to realize the synthesis of DFF from fructose, two consecutive steps were applied for the conversion of fructose into DFF (Scheme 3). Firstly, the dehydration of fructose was performed in the presence of Fe₃O₄@SiO₂-SO₃H under an



Scheme 3. Consecutive conversion of fructose into DFF.

air atmosphere. The HMF yield increased gradually, and the maximum HMF yield of 90.1% was obtained after 2.5 h at 110 °C (Figure 4). The reaction solution was separated readily from $\text{Fe}_3\text{O}_4@\text{SiO}_2-\text{SO}_3\text{H}$ with a permanent magnet, and $\gamma\text{-Fe}_2\text{O}_3@\text{HAP-Ru}$ was added into the resultant reaction solution. The oxidation reaction was performed under O_2 . The HMF content decreased gradually, and the DFF yield increased gradually (Figure 7). After 24 h, a high DFF yield of 79.1% was obtained from fructose.

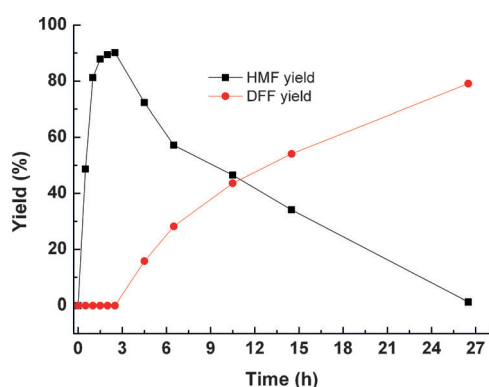


Figure 7. Conversion of fructose into DFF by two consecutive steps. Reaction conditions: First step: Fructose (143 mg, 0.8 mmol) was dissolved in DMSO (1 mL) and 4-chlorotoluene (4 mL), $\text{Fe}_3\text{O}_4@\text{SiO}_2-\text{SO}_3\text{H}$ (150 mg) was added to the mixture, and the reaction was performed at 110 °C. Second step: $\gamma\text{-Fe}_2\text{O}_3@\text{HAP-Ru}$ (150 mg) was added to the reaction solution, and the oxidation reaction was performed with an O_2 flow rate of 20 mLmin⁻¹.

Catalyst recycling experiments

The recycling of the $\gamma\text{-Fe}_2\text{O}_3@\text{HAP-Ru}$ catalyst was studied. The aerobic oxidation of HMF was used as a model reaction. The reaction was performed at 90 °C with 150 mg of $\gamma\text{-Fe}_2\text{O}_3@\text{HAP-Ru}$. After the reaction, the $\gamma\text{-Fe}_2\text{O}_3@\text{HAP-Ru}$ catalyst was separated easily from the reaction mixture with a permanent magnet (Figure 8). The catalyst was washed with water and ethanol and dried at 80 °C overnight in a vacuum oven. The spent catalyst was used for the second cycle, and the reaction was performed under the same DFF conditions. Other cycles were also performed as described above. The DFF yields remained stable (Figure 9), which indicated that there was no significant loss of the catalytic activity.

Conclusions

We have developed an efficient and environmentally benign method for the aerobic oxidation of 5-hydroxymethylfurfural (HMF) to 2,5-diformylfuran (DFF) over a magnetic catalyst composed of $\gamma\text{-Fe}_2\text{O}_3$ encapsulated with Ru-exchanged hydroxy-

apatite ($\gamma\text{-Fe}_2\text{O}_3@\text{HAP-Ru}$). A high DFF yield of 89.1% and an HMF conversion of 100% were obtained under the optimal reaction conditions. Importantly, the synthesis of DFF from fructose was achieved by acid-catalyzed dehydration and subsequent aerobic oxidation in a two-step reaction. Two consecutive steps gave DFF in a 79.1% yield. Both the magnetic acid catalyst functionalized with sulfonic acid ($\text{Fe}_3\text{O}_4@\text{SiO}_2-\text{SO}_3\text{H}$) and $\gamma\text{-Fe}_2\text{O}_3@\text{HAP-Ru}$ could be separated easily from the reaction solution with a permanent magnet and reused several times without significant loss of their catalytic activity. This method shows potential in the conversion of abundant carbohydrates into valuable bulk chemicals.

Experimental Section

Materials

$\text{FeSO}_4\cdot 7\text{H}_2\text{O}$ (99.5%), $\text{FeCl}_3\cdot 6\text{H}_2\text{O}$ (99.5%), tetraethoxysilane (TEOS, 99.5%), $\text{Ca}(\text{NO}_3)_2\cdot 4\text{H}_2\text{O}$, and $(\text{NH}_4)_2\text{HPO}_4$ were purchased from Sino-pharm Chemical Reagent Co., Ltd. (Shanghai, China). $\text{RuCl}_3\cdot x\text{H}_2\text{O}$ (38.0–42.0% Ru basis) and γ -mercaptopropyltrimethoxysilane (MPTMS) were purchased from Aladdin Chemicals Co. Ltd. (Beijing, China). Fructose was purchased from Sanland-Chem International Inc. (Xiamen, China). HMF (98%) was purchased from Beijing Chemicals Co. Ltd. (Beijing, China). DFF was purchased from the

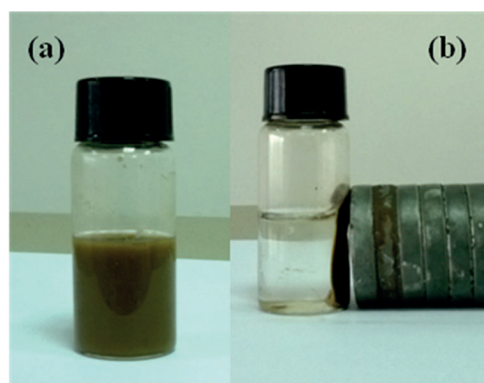


Figure 8. Separation of the catalyst: (a) After reaction and (b) separation using a permanent magnet.

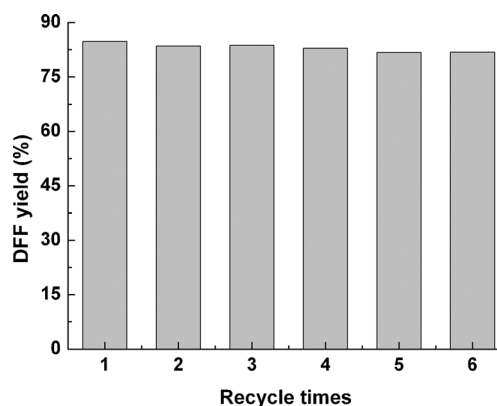


Figure 9. Recycling of $\gamma\text{-Fe}_2\text{O}_3@\text{HAP-Ru}$.

J&K Chemical Co. Ltd. (Beijing, China). Acetonitrile (HPLC grade) was purchased from Tedia Co. (Fairfield, USA). All other reagents were purchased from local supplies (Wuhan, China). All the solvents were freshly distilled before use.

Preparation of γ -Fe₂O₃@HAP-Ru

Fe₃O₄ nanoparticles were prepared and characterized as described in our previous work by the coprecipitation of Fe²⁺ and Fe³⁺ in an alkaline solution under N₂.^[27] γ -Fe₂O₃@HAP was prepared in situ without the separation of Fe₃O₄ nanoparticles. After the formation of Fe₃O₄ nanoparticles, a solution (100 mL) of Ca(NO₃)₂·4H₂O (7.95 g, 33.7 mmol) and (NH₄)₂HPO₄ (2.64 g, 20 mmol) adjusted to pH 11 were added dropwise to the obtained Fe₃O₄ nanoparticles over 30 min with mechanical stirring. The resulting mixture was heated at 90 °C for 2 h. Then the mixture was cooled to RT and aged overnight. The dark brown precipitate was separated with a permanent magnet, washed repeatedly with deionized water until a neutral solution was obtained, and dried at 60 °C overnight under vacuum. The as-synthesized sample was calcined at 300 °C for 3 h, and a reddish-brown powder (γ -Fe₂O₃@HAP) was obtained.

The cation exchange of Ca²⁺ in γ -Fe₂O₃@HAP was performed by the reaction of γ -Fe₂O₃@HAP (1.0 g) with an aqueous RuCl₃·xH₂O solution (40 mL, 5.0 × 10⁻³ M) at RT for 24 h. The catalyst was separated with a permanent magnet, washed repeatedly with deionized water until no Ru was detected, and dried under vacuum overnight. The obtained catalyst was denoted as γ -Fe₂O₃@HAP-Ru, and the content of Ru was determined to be 2 wt%.

Preparation of sulfonic acid groups

Silica-coated Fe₃O₄ nanoparticles (Fe₃O₄@SiO₂) were prepared and characterized as described in our previous work.^[27] Supported sulfonic acid was prepared by the oxidation of surface thiol groups.^[3] To a solution of MPTMS (1 g) in ethanol (10 mL) and water (10 mL) was added Fe₃O₄@SiO₂ (250 mg). The mixture was sonicated for 15 min and stirred under reflux overnight. The Fe₃O₄@SiO₂-supported thiol (Fe₃O₄@SiO₂-SH) was recovered magnetically and washed three times with water (20 mL). Fe₃O₄@SiO₂-SH was oxidized with H₂O₂ (10 mL, 30%) in a mixed solution of water (10 mL) and ethanol (10 mL) at RT overnight. The product was recovered magnetically, washed three times with water (20 mL), and reacidified with H₂SO₄ (10 mL, 0.1 M). Fe₃O₄@SiO₂ modified with sulfonic acid (Fe₃O₄@SiO₂-SO₃H) was washed three times with water and dried under vacuum at RT overnight.

Catalyst characterization

All XRD patterns were collected in the 2 θ range of 10–80° with a scanning rate of 0.016° s⁻¹.

TEM images were obtained by using an FEI Tecnai G²-1-20 instrument. The sample powder was dispersed in ethanol and dropped onto a copper grid for observation.

FTIR spectra were recorded by using a Nicolet NEXUS-6700 FTIR spectrometer with a spectral resolution of 4 cm⁻¹ in the wave number range of 500–4000 cm⁻¹. Powder XRD patterns of samples were determined by using a Bruker advance D8 powder diffractometer (CuK α).

XPS was conducted by using a Thermo VG scientific ESCA Multi-Lab-2000 spectrometer with a monochromatized AlK α source

(1486.6 eV) at a constant analyzer pass energy of 25 eV. The BE was estimated to be accurate within 0.2 eV. All BEs were corrected with reference to the C 1s peak (BE = 284.9 eV) of carbon contaminants as an internal standard.

Magnetization measurements were performed by using a physical property measurement system (PPMS-9T) with VSM option from Quantum Design. Applied magnetic fields H between –30 and 30 kOe at 300 K were used in the experiments.

Aerobic oxidation of HMF under atmospheric pressure

In a typical run, HMF (1 mmol, 126 mg) was dissolved in 4-chlorotoluene (7 mL) with magnetic stirring. γ -Fe₂O₃@HAP-Ru was added into the reaction mixture, pure O₂ was flushed at a rate of 20 mL min⁻¹ from the bottom of the reactor, and the reaction was performed at 110 °C. The mechanical stirrer was set at a constant rate of 600 rpm. The point at which O₂ was flushed into the reaction mixture was taken to be $t=0$. After reaction, the Fe₂O₃@HAP-Ru catalyst was separated from the reaction mixture with a permanent magnet, and the products were analyzed by HPLC.

Details of the use of an O₂ balloon are as follows: The air in the reaction system was expelled by a flush of pure O₂. The top of the reactor equipped with a condenser was sealed with an O₂ balloon. The volume of O₂ in the balloon was approximately 800 mL, which was far larger than the stoichiometric amount of O₂ required for the oxidation of HMF into DFF.

The procedure of the oxidation of HMF in the air was almost the same with a flush of O₂ and the reaction system was exposed to the air.

Synthesis of DFF from fructose by two consecutive reactions

Firstly, the dehydration of fructose was performed. Briefly, fructose (0.8 mmol, 143 mg) was dissolved in 4-chlorotoluene (4 mL) and DMSO (1 mL) at 110 °C. Then Fe₃O₄@SiO₂-SO₃H (150 mg) was added into the reaction solution to promote the dehydration of fructose into HMF at 110 °C for 2.5 h. After the formation of HMF, Fe₃O₄@SiO₂-SO₃H was separated from the reaction solution with a permanent magnet, and HMF in the resultant reaction solution was further oxidized to DFF with O₂ catalyzed by γ -Fe₂O₃@HAP-Ru. The procedure of the oxidation reaction was as described above.

Analytical methods

HMF and DFF were analyzed by using a VARIAN ProStar 210 HPLC system. Samples were separated by a reversed-phase C₁₈ column (200 × 4.6 mm) with a detection wavelength of 280 nm. The mobile phase was acetonitrile and 0.1 wt% acetic acid aqueous solution (30:70 v/v) at 1.0 mL min⁻¹. The column oven temperature was kept at 25 °C. The contents of HMF and DFF in samples were calculated by the external standard calibration curve method, for which the calibration curves were constructed based on the pure compounds.

Acknowledgements

This project was supported by the National Natural Science Foundation of China (Nos. 21203252, 21373275), the Natural Science Foundation of Hubei Province of China (No. 2012FFB07405), and

the Chenguang Youth Science and Technology Project of Wuhan City (No. 2014070404010212).

Keywords: multicomponent reactions · oxidation · renewable resources · ruthenium · supported catalysts

- [1] F. Rizzi, N. J. van Eck, M. Frey, *Renewable Energy* **2014**, *62*, 657–671.
- [2] C. Angelici, B. M. Weckhuysen, P. C. A. Bruijninx, *ChemSusChem* **2013**, *6*, 1595–1614.
- [3] A. Q. Liu, B. Liu, Y. M. Wang, R. S. Ren, Z. H. Zhang, *Fuel* **2014**, *117*, 68–73.
- [4] E. de Jong, A. Higson, P. Walsh, M. Wellisch, *Biofuels Bioprod. Biorefin.* **2012**, *6*, 606–624.
- [5] Z. H. Zhang, Y. M. Wang, Z. F. Fang, B. Liu, *ChemPlusChem* **2014**, *79*, 233–240.
- [6] B. Liu, Z. H. Zhang, *RSC Adv.* **2013**, *3*, 12313–12319.
- [7] J. D. Martínez, A. Veses, A. M. Mastral, R. Murillo, M. V. Navarro, N. Puy, A. Artigues, J. Bartrolí, T. García, *Fuel Process. Technol.* **2014**, *119*, 263–271.
- [8] R.-J. van Putten, J. C. van der Waal, E. de Jong, C. B. Rasrendra, H. J. Heeres, J. G. de Vries, *Chem. Rev.* **2013**, *113*, 1499–1597.
- [9] J. B. Binder, R. T. Raines, *J. Am. Chem. Soc.* **2009**, *131*, 1979–1985.
- [10] K. D. Vigier, A. Benguerba, J. Barrault, F. Jerome, *Green Chem.* **2012**, *14*, 285–289.
- [11] B. Liu, Z. H. Zhang, Z. K. Zhao, *Chem. Eng. J.* **2013**, *215–216*, 517–521.
- [12] Z. F. Fang, B. Liu, J. J. Luo, Y. S. Ren, Z. H. Zhang, *Biomass Bioenergy* **2014**, *60*, 171–177.
- [13] S. H. Xiao, B. Liu, Y. M. Wang, Z. F. Fang, Z. H. Zhang, *Bioresour. Technol.* **2014**, *151*, 361–366.
- [14] O. Casanova, S. Iborra, A. Corma, *ChemSusChem* **2009**, *2*, 1138–1144.
- [15] A. Villa, M. Schiavoni, S. Campisi, G. M. Veith, L. Prati, *ChemSusChem* **2013**, *6*, 609–612.
- [16] X. Tong, Y. Ma, Y. Li, *Appl. Catal. A* **2010**, *385*, 1–13.
- [17] Z. H. Zhang, B. Liu, K. L. Lv, J. Sun, K. J. Deng, *Green Chem.* **2014**, *16*, 2762–2770.
- [18] A. Gandini, *Green Chem.* **2011**, *13*, 1061–1083.
- [19] A. S. Amarasekara, D. Green, E. McMillan, *Catal. Commun.* **2008**, *9*, 286–288.
- [20] F. W. Lichtenthaler, *Acc. Chem. Res.* **2002**, *35*, 728–737.
- [21] O. Casanova, A. Corma, S. Iborra, *Top. Catal.* **2009**, *52*, 304–314.
- [22] W. Partenheimer, V. V. Grushin, *Adv. Synth. Catal.* **2001**, *343*, 102–111.
- [23] H. J. Yoon, J. W. Choi, H. S. Jang, J. K. Cho, J. W. Byun, *Synlett* **2011**, *2*, 165–168.
- [24] A. Takagaki, M. Takahashi, S. Nishimura, K. Ebitani, *ACS Catal.* **2011**, *1*, 1562–1565.
- [25] I. Sádaba, Y. Y. Gorbanev, S. Kegnaes, S. S. R. Putluru, R. W. Berg, A. Riisager, *ChemCatChem* **2013**, *5*, 284–293.
- [26] Y. M. Wang, B. Liu, K. C. Huang, Z. H. Zhang, *Ind. Eng. Chem. Res.* **2014**, *53*, 1313–1319.
- [27] S. G. Wang, Z. H. Zhang, B. Liu, J. L. Li, *Catal. Sci. Technol.* **2013**, *3*, 2104–2112.
- [28] T. Hara, T. Kaneta, K. Mori, T. Mitsudome, T. Mizugaki, K. Ebitani, K. Kaneda, *Green Chem.* **2007**, *9*, 1246–1251.
- [29] M. Sheykhan, L. Ma'mani, A. Ebrahimi, A. Heydari, *J. Mol. Catal. A* **2011**, *335*, 253–261.
- [30] K. Yamaguchi, K. Mori, T. Mizugaki, K. Ebitani, K. Kaneda, *J. Am. Chem. Soc.* **2000**, *122*, 7144–7145.
- [31] R. A. D. Betta, *J. Catal.* **1974**, *34*, 57–60.
- [32] C. S. Gill, B. A. Price, C. W. Jones, *J. Catal.* **2007**, *251*, 145–152.
- [33] X. Y. Sheng, J. R. Gao, L. Han, Y. X. Jia, W. J. Sheng, *Microporous Mesoporous Mater.* **2011**, *143*, 73–77.
- [34] C. He, T. Sasaki, Y. Shimizu, N. Koshizaki, *Appl. Surf. Sci.* **2008**, *254*, 2196–2202.
- [35] Y. J. Zhang, J. H. Wang, J. Yin, K. F. Zhao, C. Z. Jin, Y. Y. Huang, Z. Jiang, T. Zhang, *J. Phys. Chem. C* **2010**, *114*, 16443–16450.
- [36] Z. P. Yang, X. Y. Gong, C. J. Zhang, *Chem. Eng. J.* **2010**, *165*, 117–121.
- [37] M. Markovic, B. O. Fowler, M. S. Tung, *J. Res. Natl. Inst. Stand. Technol.* **2004**, *109*, 553–558.
- [38] Z. H. Cheng, A. Yasukawa, K. Kandori, T. Ishikawa, *J. Chem. Soc. Faraday Trans.* **1998**, *94*, 1501.
- [39] G. Kataby, A. Ulman, M. Cojocarua, A. Gedanken, *J. Mater. Chem.* **1999**, *9*, 1501–1506.
- [40] *Handbook of X-ray Photoelectron Spectroscopy* (Eds.: C. D. Wagner, G. E. Muilenberg), Perkin–Elmer Corporation, **1979**.
- [41] K. Mori, S. Kanai, T. Hara, T. Mizugaki, K. Ebitani, K. Jitsukawa, K. Kaneda, *Chem. Mater.* **2007**, *19*, 1249–1256.
- [42] S. Wuyts, D. E. De Vos, F. Verpoort, D. Depla, R. De Gryse, P. A. Jacobs, *J. Catal.* **2003**, *219*, 417–424.
- [43] C. Reichardt, *Solvents and Solvent Effects in Organic Chemistry*, 3rd ed., Wiley-VCH, Weinheim, **2003**, p. 471.
- [44] R. R. Sever, T. W. Root, *J. Phys. Chem. B* **2003**, *107*, 4080–4089.
- [45] P. Lignier, S. Mangematin, F. Morfin, J. Rousset, V. Caps, *Catal. Today* **2008**, *138*, 50–54.
- [46] Z. Opre, D. Ferri, F. Krumeich, T. Mallat, A. Baiker, *J. Catal.* **2006**, *241*, 287–295.
- [47] Z. Hu, B. Liu, Z. H. Zhang, *Ind. Crops Prod.* **2013**, *50*, 264–269.
- [48] Z.-Z. Yang, J. Deng, T. Pan, *Green Chem.* **2012**, *14*, 2986–2989.
- [49] A. W. Heinen, J. A. Peters, H. van Bekkum, *Carbohydr. Res.* **1997**, *304*, 155–164.

Received: May 10, 2014

Revised: June 11, 2014

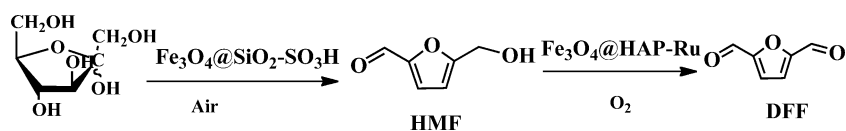
Published online on ■■■■■, 0000

FULL PAPERS

Z. H. Zhang,* Z. L. Yuan, D. G. Tang,
Y. S. Ren, K. L. Lv, B. Liu



**Iron Oxide Encapsulated by
Ruthenium Hydroxyapatite as
Heterogeneous Catalyst for the
Synthesis of 2,5-Diformylfuran**



Magnetic attraction: We have demonstrated an efficient and environmentally benign magnetic catalyst for the aerobic oxidation of 5-hydroxymethylfurfural

(HMF) to 2,5-diformylfuran (DFF). A high DFF yield of 89.1% and an HMF conversion of 100% were obtained after 4 h at 90 °C.